

Electronic structure of the complex alkali-transition-metal ternary hydrides A_2TH_4 ($A=Na, K$; $T=Pd, Pt$)

Emilio Orgaz

Departamento de Física y Química Teórica, Facultad de Química, Universidad Nacional Autónoma de México, Código Postal 04510, México, Distrito Federal, Mexico

(Received 30 April 2007; revised manuscript received 11 July 2007; published 22 October 2007)

The role of the alkali metal in determining the stability of the A_2TH_4 ($A=Na, K$; $T=Pd, Pt$) hydrides has been investigated. We computed *ab initio* the structural and electronic properties of these compounds with special emphasis on the polarizability of the counterions. We evaluated the stabilizing effect of the alkali metal by computing the H site energy. We estimated that the stabilizing effect of the K cation in these systems is 0.3–0.4 eV/H. In addition, we found that the electric field gradient at the alkali metals strongly differs from K_2PdH_4 to K_2PtH_4 , suggesting the necessity of nuclear quadrupole resonance measurements.

DOI: 10.1103/PhysRevB.76.153105

PACS number(s): 71.15.Nc, 71.20.Dg, 71.20.Ps

Ternary hydrides composed of anionic transition metal–hydrogen units and alkali metals, alkaline earth, or lanthanides exhibit a wide range of H coordinations and crystal structures.^{1,2} The large variety of the electronic and magnetic properties shown by this kind of solids has been reported in several reviews.³ One of the most interesting aspects of these compounds is the relative stability of the different known phases. The understanding of the bonding properties and, as a consequence, the stability of ternary hydrides should help to design new property oriented materials. The case of the A_2TH_4 ($A=Na, K$; $T=Pd, Pt$) hydrides attracted our interest owing to the singular ordering of the square planar TH_4 units^{4–7} and the relative stability of these phases. The A_2PdH_4 hydrides exhibit a body centered tetragonal structure (I_4/mmm). In particular, the Pt-based compounds crystallize in two different structures belonging to closely related space groups. While the Na_2PtH_4 hydride belongs to the I_4/mmm space group, the K_2PtH_4 compound crystallizes in $P4_2/mnm$ at temperatures below 195 K.⁵ The main difference in both solids is the orientation of the PtH_4 units as can be appreciated in Fig. 1. The K_2PtH_4 hydride exhibits a high temperature phase characterized by the high mobility of the PtH_4 units, which, on average, yield a face-centered-cubic structure ($Fm\bar{3}m$ space group). Although the electronic structure of these compounds is strongly dominated by the TH_4 subunits, it has been previously pointed out^{7,8} that the stability and different orientations of the TH_4 units depend on the fine specificities of the alkali cations. In this work, we investigated in detail the role of the alkali metal in determining the stability of these phases.

Electronic structure computations were carried out, employing the generalized gradient approximation⁹ to the density functional theory (DFT). Geometry optimizations of the crystal structures were obtained by means of a pseudopotential scheme. The projected-augmented plane wave method was used¹⁰ (VASP code). Suitable pseudopotentials were employed, introducing semicore states for the alkali metals and a large energy cutoff for the hydrogen atoms. We fully relaxed the spatial group constraints in order to increase the degrees of freedom during the optimizations. Geometry equilibria is obtained when a minimum is reached in total energy and local forces are 10^{-3} eV/Å. This set of computations were completed by the *ab initio* calculation of the electronic

structure of the previously optimized structures by means of the all-electron full-potential linear augmented plane waves (LAPW) method¹¹ (WIEN code). The muffin-tin radii were set to 2.00, 1.80, and 1.0 a.u. for the alkali metal, transition metal, and hydrogen atoms, respectively. The RK_{max} parameter, which controls the plane wave expansion, was selected in order to obtain converged eigenvalues up to 10^{-4} eV ($RK_{max}=5$). Additional DFT molecular computations were carried out for the alkali metals and their cations with the 6-311++G(3df,3pd) basis set and the generalized gradient approximation to the density functional.^{9,12} For the $Pt(Pd)H_4^{2-}$ anions, the LANL2DZ pseudopotential basis was employed.

It is important to note that the PdH_4 as well as PtH_4 anions exhibit a strong covalency.^{7,8} In transition metal hydrides, the well known π -backdonation stabilizing mechanism is not operative. As a consequence, the highly diffuse and polarizable H 1s orbitals play a major role. The observed high diffusivity of H atoms at moderate temperatures cannot involve a change in the local symmetry of the TH_4^{2-} units. In the high temperature phase of K_2PtH_4 , the H atoms are supposed to be randomly distributed among the six sites of an octahedra surrounding the transition metal atom. As we confirmed by means of state-of-the-art quantum molecular computations,¹² deviations of one H atom from the D_{4h} square-planar geometry in PtH_4^{2-} are not energetically plausible. For example, a C_{2v} configuration for PtH_4^{2-} —plane to axial migration of a H atom in the associated octahedra—implies a loss of energy of 1.22 eV. However, the concerted migration of two opposite H atoms from the plane to the axial positions preserves the square-planar geometry and exhibits a null energy cost. In the solid, we expect that this concerted migration involves a small energy barrier. From this, we conclude that the local disorder concerns the whole TH_4 unit without a change in the local symmetry. This kind of H mobility is expected in the high temperature phase of K_2PtH_4 hydride.

In Table I, we summarize our results of the full geometry optimization for the four hydrides under investigation. We indicate the lattice parameters as well as some of the most representative interatomic distances. As can be appreciated, the percent shift from the experimental values remains small for all the compounds. This trend is followed by the atomic

TABLE I. Structural parameters obtained after geometry optimization for the A_2TH_4 ($A=Na, K$; $T=Pt, Pd$) hydrides using the pseudopotential scheme. The percent shift with respect to the experimental reported data is indicated in parentheses. Band gap energies (eV) are reported as obtained from PAW (Δ_{PAW}) and LAPW (Δ_{LAPW}) computations.

	Na_2PdH_4	K_2PdH_4	Na_2PtH_4	K_2PtH_4
a	5.2481 (-1.65)	5.7719 (-1.01)	5.1897 (-1.22)	5.6199 (0.68)
c	6.4787 (-2.08)	7.6313 (-0.79)	6.5951 (-2.76)	8.1038 (1.01)
$d(T-H)$	1.66 (2.92)	1.67 (2.46)	1.66 (1.78)	1.66 (5.32)
$d(A-H)$	2.47 (-1.94)	2.82 (-1.19)	2.47 (-1.87)	2.83 (-0.60)
$d(T-T)$	4.93 (-1.87)	5.59 (-0.90)	4.93 (-1.91)	5.62 (0.72)
Δ_{PAW}	2.39	2.77	2.31	3.30
Δ_{LAPW}	2.25	2.72	2.18	3.34

positions which are found to be close to the neutron diffraction results (Table II). However, for the K_2PtH_4 hydride, we found Pt-H distances larger than those observed experimentally (1.58 Å) and similar to those found for the remaining A_2TH_4 hydrides. Owing to the general good agreement of our results with the crystallographic data, we suggest that the crystal structure of this particular hydride should be reinvestigated. In Table III, we show the relative total energies for the full geometry optimized solids constrained to two space groups: I_4/mmm and $P4_2/mnm$. As can be appreciated, the results for the Na-based hydrides indicate that the experimentally observed I_4/mmm structure is slightly more stable than the $P4_2/mnm$ one. The K-based hydrides show a different behavior; while the experimentally observed structure for K_2PtH_4 ($P4_2/mnm$) appears to be more stable, the K-Pd hydride shows an equivalent total energy in both structures. Once again, the general good agreement of our results with experimental data indicates that an entropic contribution should be responsible for the stabilization of these structures. This is reasonable owing to the possible disorder of the TH_4

TABLE II. Atomic positions after PAW optimization for the A_2TH_4 ($A=Na, K$; $T=Pt, Pd$). The atomic positions for T atoms are always (0,0,0). In the A_2PdH_4 and K_2PdH_4 hydrides, A atoms are located at $(1/2, 0, 1/4)$ and the H-atom positions are at $(x, x, 0)$. For the K_2PtH_4 hydride, the A atoms are at $(0, 1/2, 1/4)$ and the H atoms at $(-x, x, 0)$ and $(0, 0, x')$. Data in parentheses are the experimental values extracted from Refs. 4–7.

	x	x'
Na_2PdH_4	0.2768 (0.2128)	
K_2PdH_4	0.2739 (0.2288)	
Na_2PtH_4	0.2960 (0.197)	
K_2PtH_4	0.2094 (0.202)	0.2053 (0.195)

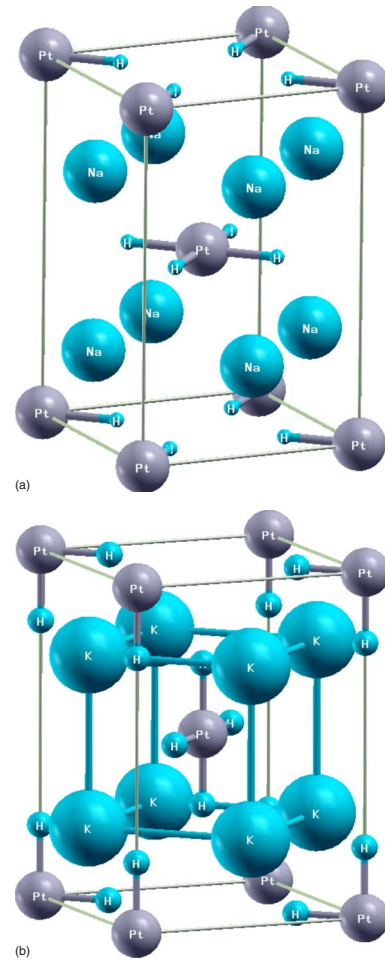


FIG. 1. (Color online) Crystal unit cells for A_2TH_4 ($A=Na, K$; $T=Pt, Pd$): (a) I_4/mmm and (b) $P4_2/mnm$.

units in both kinds of crystal arrangements. If we consider only configurational contributions to the entropy, this result should indicate that the entropy associated with $P4_2/mnm$ should be larger than that of I_4/mmm ; we do not expect a strong difference arising from this term. However, the vibrational entropy should yield a non-negligible contribution large enough to explain the stabilization of the K_2PdH_4 (I_4/mmm) phase. This matter has been recently discussed by Frankcombe.¹³

The main features of the electronic structure of these compounds have been previously investigated within a low theory level. In spite of the methodology employed, the main

TABLE III. Relative total energies ΔE (eV/f.u.) for the hypothetical $I_4/mmm \rightarrow P4_2/mnm$ transformation in A_2TH_4 ($A=Na, K$; $T=Pt, Pd$). Electric-field gradient (EFG) (10^{21} V/m²) for each element.

	ΔE	EFG A	EFG T	EFG H
Na_2PdH_4	0.132	-0.266	24.746	0.867
K_2PdH_4	-0.004	-1.104	23.558	0.881
Na_2PtH_4	0.159	-0.232	86.287	1.084
K_2PtH_4	-0.357	0.707	85.549	1.119

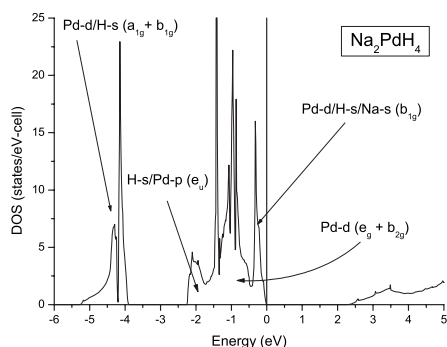


FIG. 2. Total density of states (in states/eV cell) for the optimized Na_2PdH_4 hydride obtained with the LAPW method.

characteristics of the electronic structure are preserved, indicating, in all cases, a strong molecular behavior. The plot of the total density of states (DOS), supported by the site projected DOS,⁸ is in good agreement with the standard molecular orbital energy diagram expected for a square-planar complex. The interpretation of the DOS needs the details of the eigenvector's values at each energy band weighted by symmetry, depending on the k point under consideration. In our analysis, we take into account this information at the center of the Brillouin zone. In general, five DOS structures can be observed (see Fig. 2). We analyze the case of the Na_2PdH_4 hydride, keeping in mind that the other hydrides show a similar ordering of substructures in the DOS. In increasing order of energy, we found an $a_{1g} \oplus b_{1g}$ structure composed of the bonding Td/Hs orbital interactions. At higher energies, the e_u Hs manifold appears, involving a small Tp contribution. These states are essentially of a nonbonding character in the first row transition metal complexes. In the present compounds, the Tp states contribute slightly to these states. The next structure in the DOS plot is composed of the narrow e_g and b_{2g} nonbonding Td states. The last structure, just below the Fermi energy, is of particular interest. These b_{1g} states are essentially of antibonding character, composed of the Td/Hs orbitals. These molecular solids are insulators as expected. The underestimated band gap energies are summarized in Table I for all the hydrides, computed with the PAW and LAPW methods. In all the compounds under investigation, a small As,p orbital contribution to these states was detected. In Fig. 3, we plotted the alkali metal site projected DOS for Na in Na_2PdH_4 and K in K_2PdH_4 . It is shown that the K s and particularly K p contributions close to the Fermi energy are stronger than those observed in the Na-based compound. This finding suggested that the role of the alkali metal in stabilizing the hydrides could be important.

We computed the H site energy ϵ_H (Refs. 14 and 15) for the $A_2\text{TH}_4$ hydrides in the ordered experimentally observed structures. This energy has been evaluated according to the decomposition reaction $A_2\text{TH}_4 \rightarrow A_2\text{TH}_{4-\delta} + \frac{\delta}{2}\text{H}_2$ ($\delta = \frac{1}{16}$). In this investigation, we set a large ($2 \times 2 \times 2$) supercell in order to avoid defect-defect interactions. The computed ϵ_H are 1.19, 1.22, 1.58, and 1.50 eV/H for Na_2PdH_4 , Na_2PtH_4 , K_2PdH_4 , and K_2PtH_4 , respectively. Although similar, the larger values for this property in the case of the K-based hydrides are indicative of stronger H interactions with respect to the Na-based systems. This stabilizing energy excess

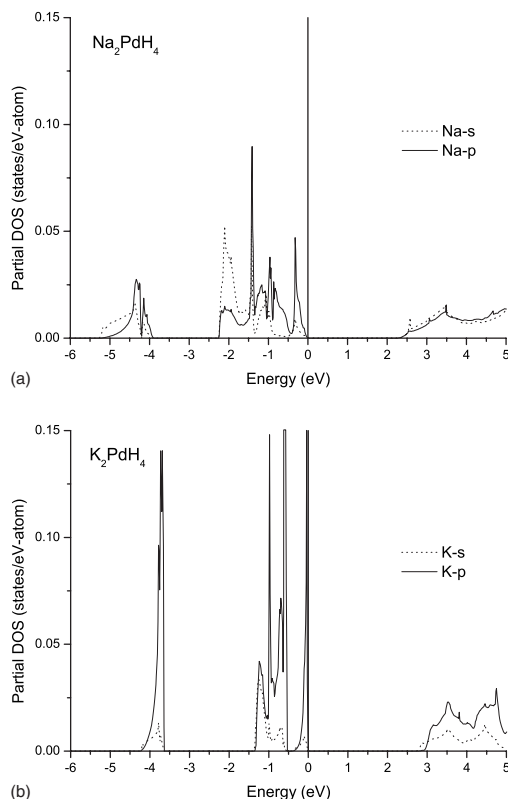


FIG. 3. Alkali metal site projected density of states (in states/eV atom). (a) Na in Na_2PdH_4 and (b) K in K_2PdH_4 , obtained with the LAPW method.

of 0.3–0.4 eV/H should arise directly from the alkali metal–hydrogen interactions. The T -H distances are similar to those found in the stoichiometric hydride; however, we were able to detect a small relaxation in the T -H distances. The Pd-H distances change from 1.66 to 1.65 and 1.68 Å, and the Pt-H from 1.66 to 1.64 and 1.68 Å. It is important to note that the local symmetry for this hydrogen defective transition metal anions is C_{2v} .

In order to explain the larger ϵ_H for the K-based hydrides and the small contributions of the alkali metals to the Fermi level b_{1g} states, we investigated the local polarizability and charge density distribution in these compounds. By means of DFT molecular methods,¹² we computed the polarizabilities α of the alkali metals, the corresponding cations, and the molecular anions $[\text{PdH}_4]^{2-}$ and $[\text{PtH}_4]^{2-}$. We found for Na, Na^+ , K, K^+ , $[\text{PdH}_4]^{2-}$, and $[\text{PtH}_4]^{2-}$ the following α values: 158.65, 0.62, 326.97, 5.57, 92.93, and 72.51 a.u.³, respectively. Our results compare well with experimental and recent theoretical studies¹⁶ for Na and K, and gives us confidence to compare the α estimates for the cations and the molecular anion. As we can appreciate, the $\alpha_K/\alpha_{\text{Na}^+}$ ratio is ≈ 2 , while for the cations, this ratio is more important $\alpha_{\text{K}^+}/\alpha_{\text{Na}^+} \approx 9$. As expected, K is twice more polarizable than Na. The Na^+ cation exhibiting a very small polarizability should conserve a spherical charge distribution in any chemical interaction. However, K^+ shows a polarizability of the same order of magnitude of, for example, rare earths and heavy alkaline earth cations, and cannot be considered marginal or negligible. It is interesting to note that the polariz-

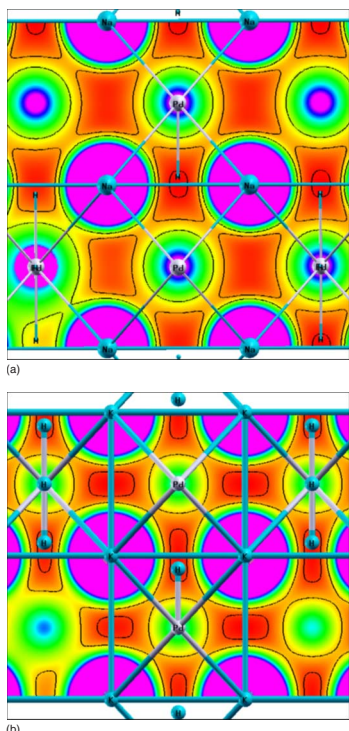


FIG. 4. (Color online) Difference charge density plots—crystal minus atomic density charge—in $e/a.u.^3$. Color scale ranges from (darker) 0.0, 0.02, 0.08, 0.18, 0.32, to 0.5 $e/a.u.^3$ (lighter). (a) Na_2PdH_4 and (b) K_2PdH_4 . Plots obtained with XCRYSDEN (Ref. 17).

abilities for H and H^- are found to be 4.09 and 11.72 $a.u.^3$. The polarizability of the molecular anion exhibits a clearly sizable value which is strongly dominated by the H atoms, which tend to show a hydrido form. We confirm these observations by inspecting the electron density charge accurately obtained from our results of all-electron solid state computation of the electronic structure. In Fig. 4, we observe the charge density plots for the Pd-derived hydrides in planes containing the alkali atoms. For the Na-based hydride, the Na atom density charge remains spherical. The K-containing compound exhibits a polarization of the semicore states toward the H sites. In addition to this observation, the K-H

distances with respect to Na-H distances are slightly larger, having in all cases an eightfold H coordination. The density charge deformation in the K-H interaction contributes to stabilizing the H site. The energy excess of 0.3–0.4 eV/H is a reasonable contribution. Supporting this, in Table III, we summarize the computed values of the electric-field gradient (EFG) at each atomic site obtained by means of the LAPW method. We observe that the EFG values for the transition metals are slightly compound dependent. However, the values of the alkali metal EFG differ greatly for both K-based hydrides while remaining similar for the Na-based compounds. This great difference between K_2PdH_4 and K_2PtH_4 could arise from the different local orientations of the TH_4 units in both structures. The H atom EFG shows a similar behavior, being smaller for the palladium-derived hydrides, which is consistent with an A-H interaction stronger in the K-based compounds. In this context, it should be interesting to reinvestigate experimentally these compounds and perform nuclear quadrupole resonance (NQR) experiments.

In conclusion, we quantitatively evaluate the relative stabilizing effect of the alkali metal by computing the H site energy by means of a diluted defect (hydrogen vacancy) creation. In this contribution, we successfully applied a theoretical approach to clarify the role of the alkali metals in stabilizing the A_2TH_4 phases. The alkali metal role was mentioned in the past, but not quantitatively evaluated. Although our results indicate some inconsistencies with previous experimental results, it is more interesting to note that, by computing the H energy site in these hydrides, we were able to distinguish the small energy effect of the counterion. The differences in the polarizabilities of both cations are of relevance in explaining the fine details of the electronic structure of these hydrides. We supported this view by inspecting the charge density distribution and the electric-field gradients computed for these compounds. We then suggest that NQR experiments could now be of particular interest in experimentally validating our findings.

Financial support was provided by DGAPA-UNAM under Grant No. IN102202. We would like to thank DGSCA-UNAM for providing us the supercomputing facilities.

¹K. Yvon, in *Encyclopedia of Inorganic Chemistry*, edited by R. B. King (Wiley, New York, 1994).

²R. B. King, *Coord. Chem. Rev.* **200**, 813 (2000).

³*Hydrogen in Metals III*, edited by H. Wipf, Topics in Applied Physics Vol. 73 (Springer, Berlin, 1997), p. 273.

⁴W. Bronger and G. Auffermann, *J. Less-Common Met.* **169**, 173 (1991); W. Bronger *et al.*, *ibid.* **142**, 243 (1988); W. Bronger *et al.*, *Z. Anorg. Allg. Chem.* **516**, 35 (1984).

⁵W. Bronger *et al.*, *J. Less-Common Met.* **116**, 9 (1986).

⁶W. Bronger and G. Auffermann, *Angew. Chem., Int. Ed. Engl.* **33**, 1112 (1994).

⁷D. Noréus, *Z. Phys. Chem., Neue Folge* **162**, 575 (1989); K. Kadir *et al.*, *J. Less-Common Met.* **172**, 36 (1991); W. Bronger and G. Auffermann, *J. Alloys Compd.* **228**, 119 (1995).

⁸E. Orgaz and M. Gupta, *J. Alloys Compd.* **253**, 326 (1997); E. Orgaz and M. Gupta, *Int. J. Quantum Chem.* **80**, 141 (2000).

⁹J. P. Perdew *et al.*, *Phys. Rev. Lett.* **77**, 3865 (1996).

¹⁰G. Kresse and J. Hafner, *Phys. Rev. B* **47**, 558 (1993); G. Kresse and J. Furthmüller, *Comput. Mater. Sci.* **6**, 15 (1996); P. E. Blöchl, *Phys. Rev. B* **50**, 17953 (1994); G. Kresse and D. Joubert, *ibid.* **59**, 1758 (1999).

¹¹P. Blaha *et al.*, WIEN2K, An Augmented Plane Wave + Local Orbitals Program for Calculating Crystal Properties (Technische Universität Wien, Austria, 2001).

¹²M. J. Frisch *et al.*, GAUSSIAN 03, Revision C.02 (Gaussian, Inc., Wallingford, CT, 2004).

¹³T. J. Frankcombe, *J. Alloys Compd.* (to be published).

¹⁴E. Orgaz and A. Aburto, *J. Chem. Phys.* **125**, 144708 (2006).

¹⁵A. Aburto and E. Orgaz, *Phys. Rev. B* **75**, 045130 (2007).

¹⁶R. W. Molof *et al.*, *Phys. Rev. A* **10**, 1131 (1974); C. Ghanmi *et al.*, *Comput. Mater. Sci.* **38**, 494 (2007); A. J. Thakkar and C. Lupinetti, *Chem. Phys. Lett.* **402**, 270 (2005).

¹⁷A. Kokalj, *J. Mol. Graphics Modell.* **17**, 176 (1999).